Braz J Phys (2015) 45:132–137
DOI 10.1007/s13538-014-0293-8

GENERAL AND APPLIED PHYSICS

Ferrite Loaded DBD Plasma Device

M. Machida

Received: 18 September 2014 / Published online: 19 December 2014

Abstract An atmospheric pressure plasma jet device with dielectric barrier discharge was built using low cost 5C22 thyratron valve and ferrite transformer. The ferrite transformer increases the intensity about four times the primary pulse and lengthens the high voltage pulse, keeping the rise time of the thyratron pulse. Spectrometer measurement shows excited nitrogen molecular emissions of second positive system. The most intense nitrogen molecular line, 357.69 nm, was chosen to monitor the time dependence of the discharge. Synthetic temperature, using 380.49 nm line of N_2 emission and SpecAir simulation, shows plasma gas temperature of 300 K. To corroborate this low temperature, the plasma jet is applied to human tongue with no harm or bad physical feeling.

Keywords DBD atmospheric plasma jet · 5C22 thyratron valve · Ferrite transformer · N_2 spectral emission · Synthetic temperature

1 Introduction

Dielectric barrier discharge (DBD) devices have been employed for the last decades to produce cold atmospheric pressure plasma jets (APPJs). These non-thermal plasmas are of particular interest due to their molecular reactive characteristics and needless of vacuum systems, working at room temperature and pressure [1, 2]. To obtain low temperature atmospheric pressure plasma using DBD device, the main technique is to provide a high voltage (HV), about 10 kV or higher, within rise time of approximately 100 ns, in small space, typically few millimeters, producing a fast local variation of electric field, about 1×10^6 V/m. This will create weakly ionized plasma, near the isolated conductor and with certain gas flow, and will produce a plasma jet driven by surface wave [3–5]. To produce fast variation high electric field, different sources as radio frequency oscillators [6], microwaves [7], high frequency square waves [8], DC discharges [9], or high frequency pulsed discharges [10], all with HV, can be used.

In this work, we have used a homemade pulse generator with a thyratron 5C22 valve, commonly used to trigger capacitor bank spark gap switches [11], but at much lower voltage of about 5 kV and high repetition rate. The 5C22 valve (www.datasheetarchive.com/5c22-datasheet.html) is well-known and is a low cost hydrogen valve triggered by 250 V pulser, and its electrical circuit is very simple. In our case, the main difference from other DBD power supply is the employment of ferrite transformers. Although starting with lower HV pulse of about 5 kV, the ferrite transformer can build up output voltage to about 20 kV, depending on turn rate between primary and secondary of the transformer. Furthermore, the ferrite transformer can work as a full isolation transformer, increasing the user security, since there is no direct electrical contact from main HV transformer source to DBD plasma source. Using the ferrite transformer, the initial 5C22 thyratron nanosecond pulse is transformed to microsecond pulse, maintaining the initial fast rise time of about 100 ns. At this moment, the repetition frequency is less than 60 Hz limited by 250 V trigger pulser; however, a pulse generator of up to 3 kHz is under construction. The cold atmospheric plasma jet produced by this novel device has synthetic temperature of 300 K obtained using SpecAir simulation code. The spectral emission from plasma plume obtained using Andor Shamrock 303i spectrometer is formed of second positive molecular nitrogen emissions, and it is possible to be applied on the human skin or more sensitive parts, as our tongue.

M. Machida (✉)
Universidade Estadual de Campinas - UNICAMP, Instituto de Física "Gleb Wataghin", Campinas, S.P. 13083-970, Brazil
e-mail: machida@ifi.unicamp.br

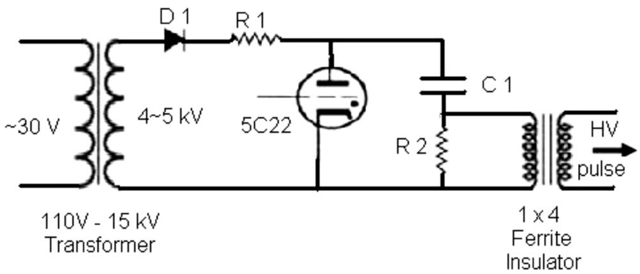

Fig. 1 High voltage pulse generator circuit using 5C22 valve with ferrite transformer and trigger pulse of 250 V is connected to grid entrance of 5C22

2 Experimental

Experimental setup is divided in HV pulse forming network, DBD plasma reactor tube, and diagnostic systems. The pulse forming network is well-known HV pulse generator built to trigger capacitor bank spark gap switches of theta-pinch machine [12], as shown in Fig. 1. Initially, input voltage of 110 V AC is reduced to about 30 to 40 V using a variac, not shown, and connected to a HV transformer (110 to 15 kV), commonly used in commercial neon lamp, to obtain output voltage of about 5 kV AC. This AC voltage is connected to HV diode for half-wave rectification. The resistor R_1 of 470 kΩ is to limit current on the transformer, and the capacitor C1 of 2.5 nF and resistor R_2 of 60 MΩ are to produce initial HV pulse output. The 5C22 hydrogen thyratron valve is a hot-cathode grid-controlled gas rectifier tube, which can be operated at high repetition frequencies, up to few kilohertz; high peak currents, maximum to 325 A; and voltage up to 16 kV, producing HV peak with fast rise time, lower than 0.5 μs. We use at this moment single pulse or pulse frequency up to 60 Hz due to our 250 V pulse generator limitation; however, frequencies up to about 1 kHz or higher can be applied according to valve specification data sheet (www.datasheetarchive.com/5c22-datasheet.html). The ferrite transformer is Mn-Zn ferrite of toroidal shape type O-5, with initial permeability of 3000, core loss at 100 kHz of 0.3 W/cm^3 and dimensions of 7.4 cm OD× 3.9 cm×1.3 cm thick [13]. The use of ferrite with lower permeability and core loss may produce higher voltage increase and faster raise time pulse. As to plasma production, there is no difference to use positive or negative HV pulse related to input pulse polarity.

Figure 2 shows a typical 5C22 pulse, with 5 kV charge on high voltage transformer. The signal is taken at resistor R_2 of 60 MΩ, using wide band pulse current transformer Pearson Electronics model 411, with no ferrite transformer. The rise time of pulse is about 100 ns, and the pulse duration is about 200 ns.

When the ferrite transformer is connected, a current will flow through the primary of the ferrite transformer, and it produces at secondary an insulated higher voltage pulse, according to primary to secondary coil turning rate. Our ferrite transformer has 1×4 coil turning rate, which gives the final high voltage pulse of about four times magnification. Figure 3 shows a pulse of 19.6 kV and pulse duration of 4 μs, measured with HV probe Tektronix P6015A. This is about ten times longer compared to initial 5C22 pulse of Fig. 2. Furthermore, the use of ferrite transformer produces plasma jet with much stronger light emission, and without use of ferrite, one must increase the HV output of main transformer to maximum of 15 kV in order to get very weak plasma plume from output of DBD plasma tube reactor.

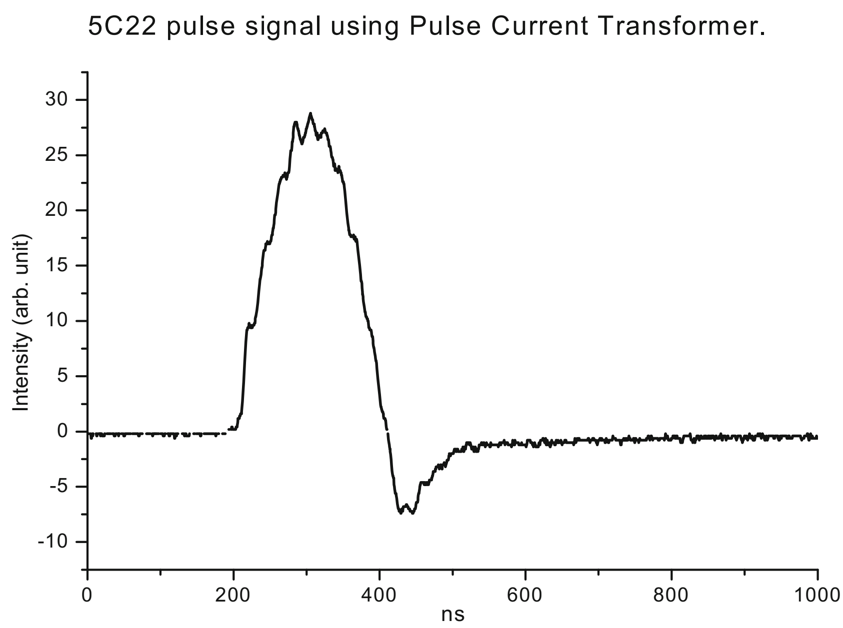

Fig. 2 Signal from 5C22 valve before ferrite transformer using fast response pulse current transformer

The main body of the plasma reactor is of coaxial type [14] as shown in Fig. 4. In this work, we have employed for the HV pulse metal rod only one fixed size, as well as for the end closed glass tube. The outer part of plasma reactor is made of polyvinyl chloride (PVC) or glass tube of different dimensions, as listed on Table 1. The glass tube has been used to allow optical access for the spectroscopic measurements of plasma produced inside reactor, since it can have distinct spectral emission from outside plasma jet [10]. The HV metal rod is connected directly to the secondary output of the ferrite transformer; however, there is no direct electrical contact between HV metal rod and plasma jet due to the dielectric end closed glass tube barrier. The plasma formation region is around the outer side of the inner glass tube surface, and the output exit hole can be replaced by different size from 2 to 6 mm. The gas flow, usually helium, of 4 to 6 l/min is controlled by a rotameter.

The He plasma jet is of pencil shape; larger plasma diameter can be defined by output hole diameter, and minimum diameter at tip of the plume is about 2 mm. The plasma plume length is typically from 2.5 to 5.0 cm according to gas flow rate, applied HV, and output hole diameter. Figure 5a–c shows three different configuration plasma jets. The metallic platform under the jet acts as ground electrode, and it is covered with some dielectric material as glass or Mylar to avoid arcing. Instead of metallic platform, some biological materials also can be used as ground reference in many cases.

Figure 5a is all PVC plastic reactor tube, and the He plasma plume is discharged on 3-mm-thick glass plate on the metallic platform. The distance from plasma output to glass plate is about 15 mm. The configuration shown in Fig. 5b has obtained higher plasma light emission and longer plasma plume, and it is used as the best configuration for power measurements. The configuration at Fig. 5c has the largest inner plasma volume and can obtain bigger plasma diameter, and it is best suited to use for inner plasma light emission measurements. As observed at Fig. 5c, plasma is produced on the external surface of the inner glass tube and travels along the tube toward the exit hole. The optical emission spectroscopy (OES) was realized at the inside glass tube and outside, at the plasma jet coming out of the plasma reactor. Two different spectrometers have been used, Andor Shamrock 303i emission spectrometer coupled to an optical fiber located perpendicularly to the plasma jet, in the range from 280 to 880 nm. The gratings of 150 or 1200 l/mm can be used, and the entrance slit was set to 200 μm. At the exit side of the spectrometer, iStar DH720 ICCD detector was employed to obtain spectral profiles of all visible spectral emissions. A second spectrometer has been set to follow temporal variation of single specific spectral molecular emission, using McPherson model 2051 1 m focal length 1200 l/mm grating, and EMI 9635B photomultiplier. The response time of photomultiplier has been checked by using red LED lamp and square wave power supply at the entrance slit of spectrometer.

The power measurements were performed using DBD device of thin glass tube configuration, Table 1, and a metallic platform under the jet, covered with glass. Typical voltage and current signals, as shown in Fig. 6, are taken simultaneously at HV pulse metal rod tip and at 47 Ω resistor set between metallic platform isolated with glass and ground.

The voltage signal is from output of HV ferrite transformer, and the current signal is from plasma discharge at bottom glass platform. As can be observed, the plasma is produced by fast variation of electric

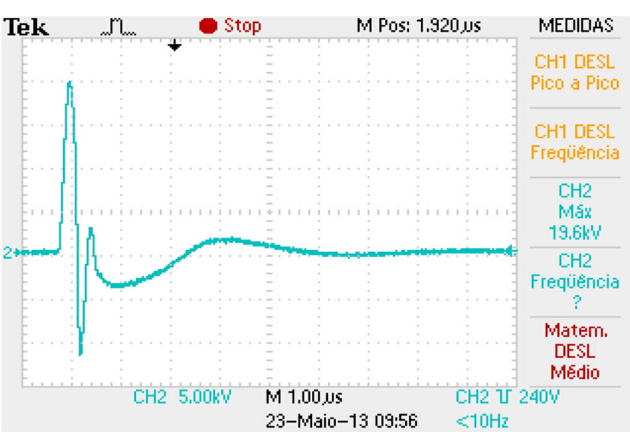

Fig. 3 Signal from output of ferrite transformer, using fast response high voltage probe

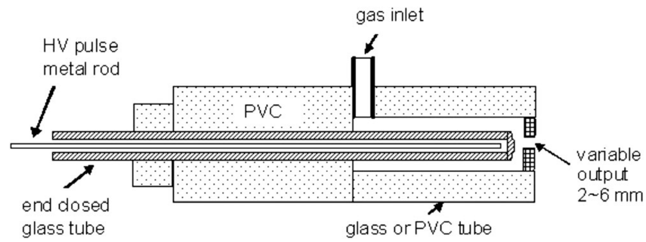

Fig. 4 Schematic view of plasma reactor; the dimensions of end closed glass tube and metal rod can be changed by changing the O-ring sealed screw nut, not shown, at the end of PVC tube

Table 1 Dimensions of coaxial DBD plasma reactor configuration

	All plastic tube (mm)	Thin glass tube (mm)	Large glass tube (mm)
External diameter	25.0	16.0	28.0
Internal diameter	15.0	12.0	22.0
Plasma cavity length	20.0	50.0	60.0
Electrode glass diameter	6.0	6.0	6.0
Electrode metal diameter	2.5	2.5	2.5

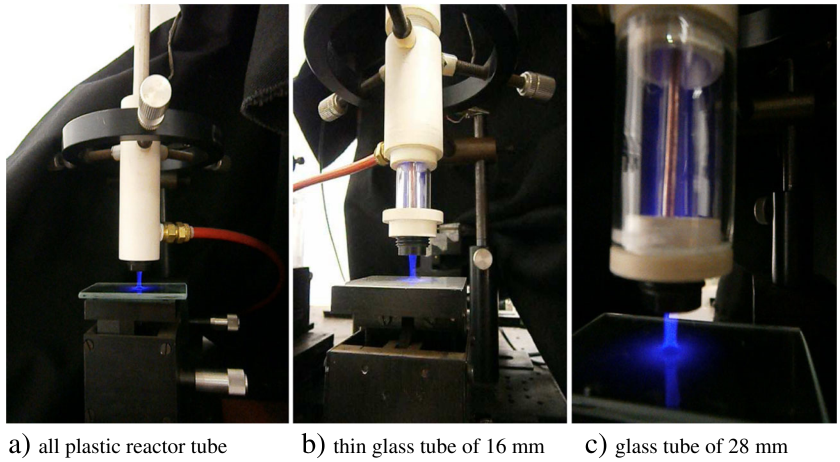

Fig. 5 **a** All plastic reactor tube. **b** Thin glass tube of 16 mm. **c** Glass tube of 28 mm

field, which is at fast increase and decrease region of voltage signal. The power measurements were done with direct integration of voltage and current signals during the time of plasma pulse duration. Using the repetition rate of 30 Hz, we obtain energy of 3.3 mJ/pulse and power delivery of 100 mW.

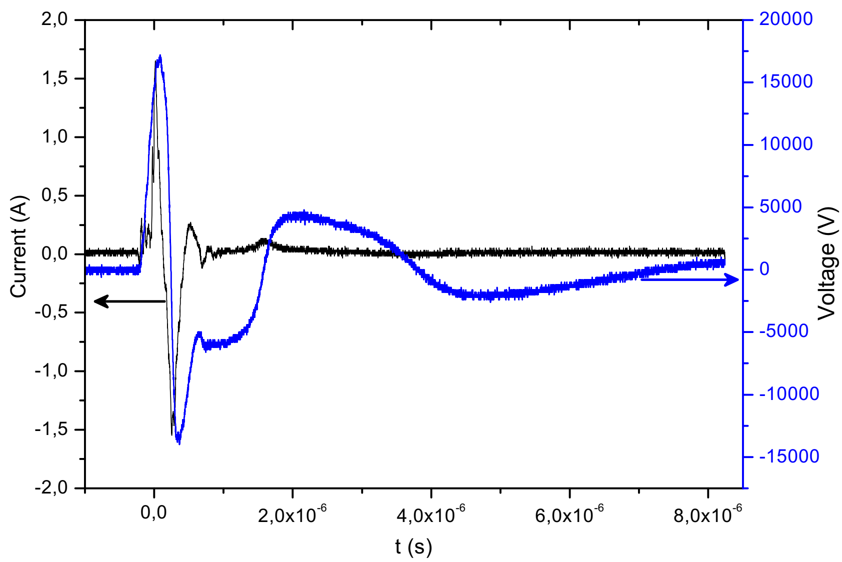

Fig. 6 Current (*left axe*) and voltage (*right axe*) signals. The *vertical axes* have been shifted to better view of signals

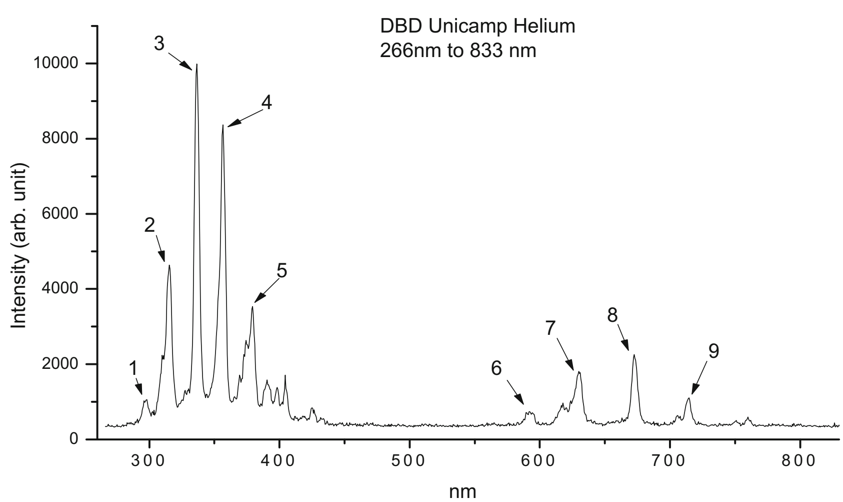

Fig. 7 Spectral emissions of plasma jet outside reactor, from 266 to 833 nm, He plasma, using Andor spectrometer with 150 l/mm grating

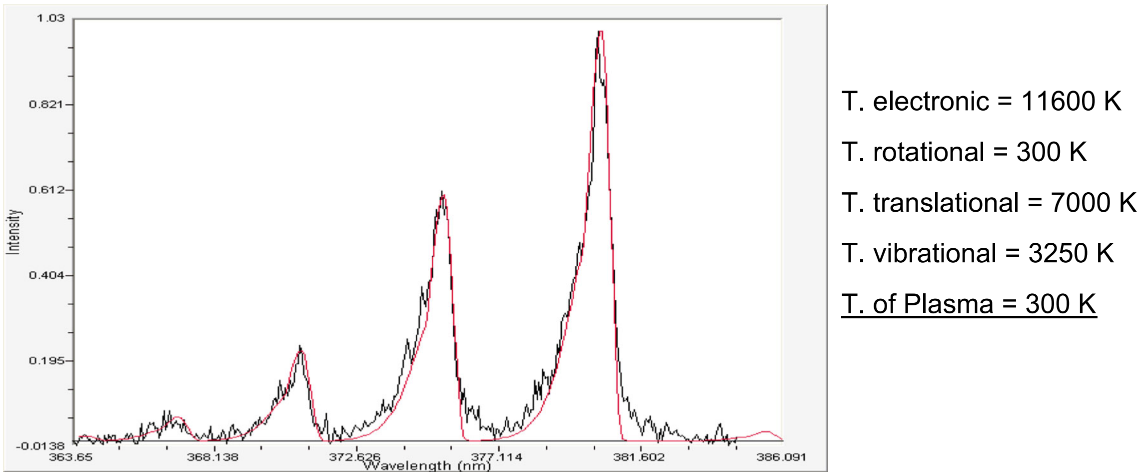

Fig. 8 Fitting of experimental data with SpecAir code simulation, of 380.49, 375.54, 371.05, and 367.19 nm emissions

3 Results

Measurements obtained from spectrometer Andor 303i, using 150 l/mm grating and iStar DH720 ICCD detector, show that spectral emissions are about the same for both, inside and outside plasma; however, the emission intensity is much stronger outside compared to inside. Spectral emissions are mainly from N_2 and OH excited and ionized molecular emissions, shown in Fig. 7. In this figure, emission near 300 nm (peak1) is from OH transition $A^2\Sigma^+$ - $X^2\Pi$ rotational, followed by second positive excited N_2 lines, $C^3\Pi_u$–$B^3\Pi_g$, at 315.93 nm (peak2), 337.13 nm (peak3), 357.69 nm (peak4), and 380.49 nm (peak5), respectively. Emissions seen from 600 to 750 nm are mostly from second-order diffraction lines, as peak7 from peak2, peak8 from peak3, and peak9 from peak4, although some HeI lines, peak6 from 587.56 nm mixed with other lines, also are present in this interval. Spectral emissions near 350 nm are useful to determine the plasma gas temperature, due to their emission intensities and isolation from other lines. Further detailed spectral emission analysis is under work.

The plasma jet produced in DBD discharges possesses different rotational, vibrational, and translational temperatures, indicating non-equilibrium conditions [15, 16]. The gas temperature at atmospheric pressure plasma can be related to thermal translational energy of the gas species, because it is of same order of magnitude of the rotational transition energy, and to short mean free path of the species [17]. Therefore, synthetic temperature is inferred by fitting experimental data and simulation [18]. In our case, as shown in Fig. 8, we use 371.05, 375.54, and 380.49 nm of second positive excited N_2 lines. The best fitting values obtained are the plasma gas temperature of 300 K related to rotational temperature, electronic temperature of 11,600 K, translational temperature of 7000 K, and vibrational temperature of 3250 K.

The time dependence of the plasma jet extracted from the plasma reactor was obtained by using 1 m McPherson spectrometer with 810 V applied to EMI 9635B photomultiplier,

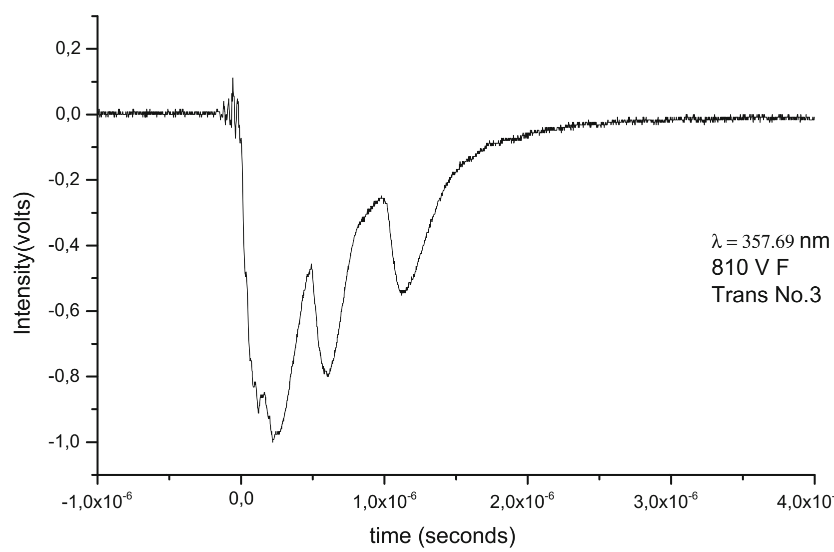

Fig. 9 Time variation of N_2II molecular emission at 357.69 nm, rise time of 200 ns and 2 μs of duration

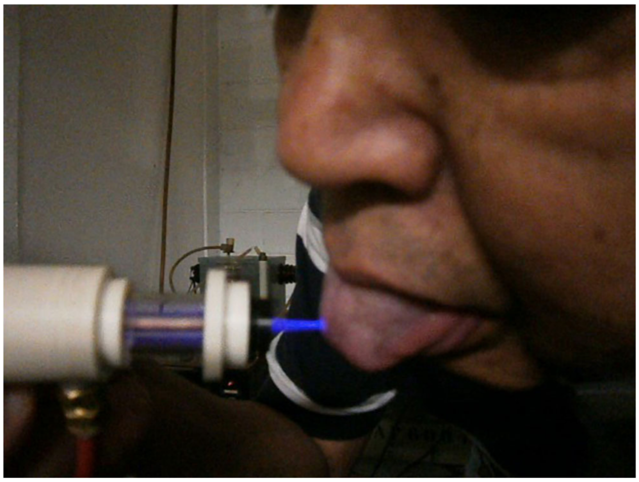

Fig. 10 Application of plasma jet at human tongue at room temperature and pressure

connected to Tektronix TDS210 oscilloscope, as shown in Fig. 9. The wavelength has been set to 357.69 nm, and we observe temporal duration of about 2.5 μs; this is half of the pulse time from ferrite transformer, and ten times the 5C22 pulse time. However, the rise time of the signal is about the same as 5C22 thyratron original pulse.

One characteristic of our APPJ plasma is room temperature plasma, so that it can be applied to biological examples as human skin, or to even much sensitive human part as our tongue as presented in Fig. 10, which corroborate to applications in plasma medicine [19–21] as an alternative low cost and safe DBD plasma device.

4 Conclusion

A low cost 5C22 thyratron valve has been used to produce 5 kV, fast rise, 200 ns pulse, and amplified by ferrite core transformer to obtain 20 kV and 2 μs atmospheric pressure plasma jet. Power measurements show up to 100 mW and 3.3 mJ/pulse for 60 Hz. At this moment, low repetition, less than 60 Hz, mode is applied; however, a higher frequency, up to 2 or 3 kHz, 250 V pulse generator is under construction. The plasma reactor is built using PVC and normal glass tubes to produce low temperature plasma plume. Three sets of geometrical configurations were employed to study OES using two different spectrometers. Spectral measurements show usual excited nitrogen molecules, mainly second positive band system, with plasma gas temperature of 300 K. To corroborate this low temperature, the plasma jet has been applied to human tongue with no harm or bad physical feeling. Our APPJ device could be useful for temperature sensitive material processing and atmospheric biological or medical treatments.

Acknowledgments The author wish to thank Dr. Vadym Prysiazhnyi, DFQ-FEG-UNESP, who helped to perform DBD power measurements, and Prof. Dr. Júlio Akashi Hernandes to localize the reference [13].

References

1. D.B. Graves, J Phys D Appl Phys **45**(263001), 42pp (2012)
2. M. Laroussi, T. Akan, Plasma Process Polym **4**, 777–788 (2007)
3. M. Chaker, M. Moisan, Z. Zakrewski, Plasma Chem Plasma Process **6**, 79–96 (1986)
4. E. Bloyet, P. Leprince, M. Llamas Brasco, J. Marec, Phys Lett **8**, 391–392 (1981)
5. O.M. Gradov, L. Stenflo, J Plasma Phys **65**, 73–77 (2001)
6. A. Yanguas-Gil, K. Focke, J. Benedikt, A. von Keudella, J of Appl Phys **101**, 103307 (2007)
7. C. Wang, N. Srivastava, Eur Phys J D **60**, 465–477 (2010)
8. J.L. Walsh, J.J. Shi, M.G. Kong, Appl Phys Lett **88**, 171501 (2006)
9. X. Pei, X. Lu, J. Liu, D. Liu, Y. Yang, K. Ostrikov, A. Paul, K. Chu, Y. Pan, J Phys D Appl Phys **45**, 165205 (2012). 5pp
10. C.B. Mello, K.G. Kostov, M. Machida, L.R.O. Hein, K.A. Campos, IEEE Trans Plasma Sci **40**, 2800–2805 (2012)
11. E.A. Aramaki, PhD thesis IF-USP, December, (1992)
12. M. Machida, S.V. Lebedev, S.A. Moshkalyov, D.O. Campos, L.A. Berni, Braz J Phys **26**, 04 (1996)
13. R. F. Gribble, Proceedings of symposium on engineering problems of fusion research, LANL, DI-5-1 TO DI-5-3, Los Alamos, N. M., (1969)
14. X. Lu, G.V. Naidis, M. Laroussi, K. Ostrikov, Physics Reports, 123–166, 540, (2014)
15. X. Lu, S. Wu, Paul K. Chu, D. Liu, Y. Pan, Plasma Sources Sci. Technol. 20 065009 (5 pp), (2011)
16. X. Lu, Y. Cao, P. Yang, Q. Xiong, Z. Xiong, Y. Xian, Y. Pan, IEEE Transactions on Plasma Science, Vol. 37, No. 5, (2009)
17. P. Bruggemann, J Phys D Appl Phys **46**, 464001 (2013)
18. http://www.specair-radiation.net/, accessed in January (2012)
19. G. E. Morfill1, M. G. Kong, J. L. Zimmermann, New J Phys, 11, 115011, 2009
20. G. Fridman, G. Friedman, A. Gutsol, A. B.. Shekhter, V.N. Vasilets, A. Fridman, Plasma Process Polym **5**, 503–533 (2008)
21. M. Vandamme, E. Robert, S. Dozias, J. Sobilo, S. Lerondel, A. Le Pape, J.M. Pouvesle, Plasma Med **1**, 27–43 (2011)